Supramolecular Chemistry
Publication details, including instructions for authors and subscription information:
http://www.informaworld.com/smpp/title~content=t713649759

Molecular dyes used for the detection of biological and environmental heavy metals: Highlights from 2004 to 2008

Karl J. Wallace[a]
[a] The University of Southern Mississippi, Hattiesburg, USA

To cite this Article Wallace, Karl J.(2009) 'Molecular dyes used for the detection of biological and environmental heavy metals: Highlights from 2004 to 2008', Supramolecular Chemistry, 21: 1, 89 — 102
To link to this Article: DOI: 10.1080/10610270802516633
URL: http://dx.doi.org/10.1080/10610270802516633

Supramolecular Chemistry
Vol. 21, Nos. 1–2, January–March 2009, 89–102

Taylor & Francis
Taylor & Francis Group

Molecular dyes used for the detection of biological and environmental heavy metals: Highlights from 2004 to 2008

Karl J. Wallace*

The University of Southern Mississippi, Hattiesburg, USA

(*Received 11 July 2008; final version received 18 September 2008*)

The coordination chemistry of heavy metals, for example, Fe^{3+}, Pb^{2+}, Cd^{2+}, Hg^{2+}, Cu^{2+} and Zn^{2+}, is of interest, in part because of their hazards and toxicity in biological, industrial and agricultural applications. Additionally, there is much interest in the detection and quantification of trace metals in the products of chemical synthesis, in particular sensors for detecting Pd^{2+}. There has been plethora of new molecular sensors for the detection of heavy metals, which utilise colorimetric or fluorescence mechanisms. This mini-review covers recent advances (2004–2008) in the development of molecular sensors that is restricted to molecular dyes. Other methods for the detection of heavy metals, for example, conjugated polymers and gold nanoparticles are omitted.

Keywords: coordination of metal; dyes; molecular recognition; host–guest chemistry; sensors

Introduction

Development of analytical tools for the detection of heavy metals, for example, Hg^{2+}, Cu^{2+}, Cd^{2+}, Zn^{2+}, Fe^{3+} and Pd^{2+}, has been a continuing endeavour. Efforts are ongoing to prepare rapid and inexpensive techniques for the detection of heavy metals and this mini-review will cover a small sample of developments from the last 4 years. A number of popular current methods for detecting the presence of heavy metals require somewhat sophisticated analytical techniques, including atomic absorption spectroscopy (*1*), mass spectroscopy (*2*), X-ray fluorescence spectroscopy (*3*, *4*) and potentiometric methods (*5*). However, these methods can be cumbersome and impractical for on-site testing and while they can be very precise, even in the ppt and ppq range, the instruments are often expensive to run. Therefore, the development of less expensive methods utilising smaller, more portable instruments for the sensitive detection of trace elements is desirable. The recognition of metals using an optical response (colorimetric and fluorescence), which is seen upon a change in the environmental stimuli, is a well-understood phenomena and the methods, which include photo-induced electron transfer (PET), fluorescence enhancement (FE) and colorimetric or 'Naked' eye detection, have been extensively reported in some excellent reviews (*6–9*).

The two most abundant trace elements in mammalian cells are iron and zinc (*10*). The majority of biomolecular iron and zinc found in nature is tied up within a number of enzymes and proteins. For example, iron is involved either in storage or transport (*11*, *12*), whereas, Zn^{2+}-containing proteins are often found in the catalytic site of an enzyme, for example, lactate dehydrogenase, which has antioxidant properties (*13–17*). Even though these trace elements are essential in mammalian cells, iron (in particular Fe^{3+}) and Zn^{2+} can both have deleterious effects. Iron(III) is found in labile iron pools, where both Fe^{2+} and Fe^{3+} oxidation states are present. Labile Fe^{3+} is a source for metabolic reactions that occur within the cell and is a site for the generation of radicals (*10*, *18*). Recent advances in cell biology have shown that not all of Zn^{2+} is incorporated in proteins, and just like Fe^{3+}, there is also a certain amount of free (or chelatable) Zn^{2+}. This is particularly true for the free Zn^{2+} that is found in the brain (*19*), pancreas (*20*) and prostate (*21*). It is believed that free Zn^{2+} is sequestered in the vesicles of presynaptic neurons and is released when the neurons are active. A problem with free Zn^{2+} detection in the cell is the low abundance, which is typically in the nanomolar range. Unfortunately, Zn^{2+} lacks any spectroscopic features due to its d^{10} configuration and cannot be monitored directly; therefore, other spectroscopic means of detection are being sought.

Iron (in the form Fe(III)) also has a significant environmental impact (*22*). The amount of Fe^{3+} exceeds that of all other bioactive metals combined in the anoxic (no oxygen present) world (*23*). As a consequence, the extremely low solubility (nM range) of Fe^{3+} in oxic (oxygen present) seawater, combined with its sparse inputs in modern times, limits plankton production of Fe^{3+}. Therefore, Fe^{3+} influences the composition of neritic

*Email: karl.wallace@usm.edu

ISSN 1061-0278 print/ISSN 1029-0478 online

DOI: 10.1080/10610270802516633
http://www.informaworld.com

algal assemblages, shifting coastal algal assemblages, impacting the structure of the ecosystem and altering the cycle and burial rates of carbon in the carbon cycle as well as negatively affecting fisheries productivity (*24–26*). Additionally, there is evidence that Fe^{3+} is the source of bloom development of a number of harmful algal species, for example, *Alexandrium tamarense* (*27*, *28*).

Mercury is another metal of interest for monitoring purposes, given its acute and chronic toxicity, which is a particular problem in aquatic systems (*29–31*). The bioaccumulation of mercury in fish is more prevalent in fish near the top of the food chain such as shark, swordfish, king mackerel, albacore tuna and tilefish.

Metals also play a pivotal role in synthesis for drug development. Palladium complexes represent some of the more useful facilitators of organic transformations known. Palladium(II) salts, such as $PdCl_2$ (*32*), $Pd(OAc)_2$ (*33*) and $PdCl_2(PPh_3)_2$ (*34*), are predominantly used as oxidising reagents, as well as precatalysts for cross-coupling reactions. Of the wide array of commonly used reactions catalyzed by these complexes, such as Suzuki, Heck and aromatic amination reactions, many processes would not be feasible or practical without the use of these metal catalysts (*35–38*). Many of these methodologies are widely utilised in pharmaceutical research and in the production of drugs (*39*), for which there are tight governmental restrictions on the levels of residual heavy metals in end products. The recommended dietary intake of palladium is $<1.5\,\mu g$/day per person and typical contamination levels of palladium remaining in the organic phase after experimental work-up range from 5 to 100 ppm (*35*). Due to its utility as well as its inherent stickiness, palladium poses a difficult challenge for both removal and detection. Optical sensing for Pd^{2+} is extremely rare: since 2004, there have only been two published papers featuring Pd^{2+} sensors (*vide infra*) (*40*, *41*) and one other in 2002 (*42*).

There are many excellent reviews in the literature that extensively cover the area of cation/heavy metal sensing, a vast subject that covers different fields of science. Many of the previously reported sensors consist of macrocyclic receptors (*43–47*). The goal of this mini-review will highlight some of the more recent developments (2004–2008) of molecular sensors for the detection of heavy metals.

Squaraine-containing receptors

The condensation reaction between 3,4-dihydroxycyclobut-3-ene-1,2-dione (squaric acid) and *N*,*N*-dialkylanilines, benzothiazoles, phenols, pyrroles and azulenes has led to an explosion of polymethine dyes that are resonance-stabilised zwitterionic structures (Scheme 1) (*48*, *49*). These dyes are now commonly referred to as 'squaraine' dyes, a name coined by Schmidt (*50*). Squaraine dyes belong to a class of chromophores that is gaining significant popularity as sensors in the field of 'supramolecular analytical' chemistry (*51*). Squaraine dyes have interesting properties and exhibit intense absorption bands (extinction coefficients (ε) of $\geq 10^5$ $cm^{-1}M^{-1}$), in the visible to near-IR regions. This absorption property is a very attractive one in sensor design, and is desirable for integration with optical instrumentation.

Recently, a good review by Ajayaghosh on the chemistry of squaraine derivatives and their use in polymer and cation sensors has been published (*49*, *52*, *53*). Much of this work has come from the laboratories of Ajayaghosh, where squaraine dyes have been incorporated into polymer networks for the development of optical materials. An elegant example of a squaraine dye used as a molecular podand has been synthesised (compound **1**), and it exhibits high selectivity for Ca^{2+} at low concentration (5.1 μM) in CH_3CN solution (*54*, *55*). It is well known that crown ethers bind group 1 and group 2 metals (*56*). Compound **1** was synthesised by appending two squaraine motifs to a polyether backbone. Upon the addition of $Ca(ClO_4)_2$, a conformational change occurred due to the coordination of Ca^{2+} to the oxygen atoms within the ether linker (Scheme 2). This conformation

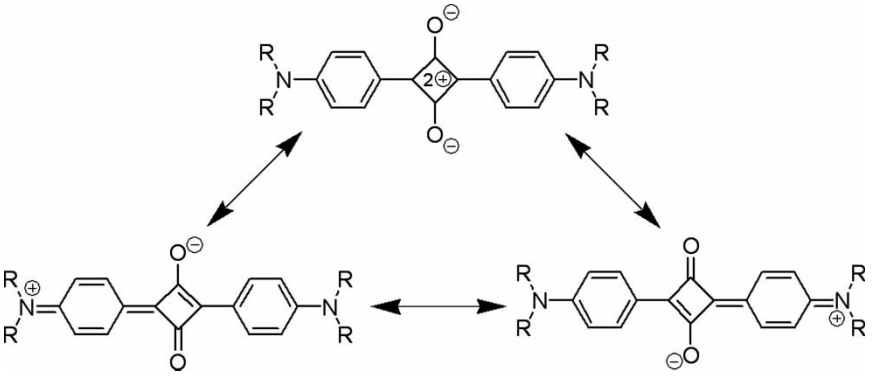

Scheme 1. Resonance-stabilised zwitterion structure of the squaraine backbone.

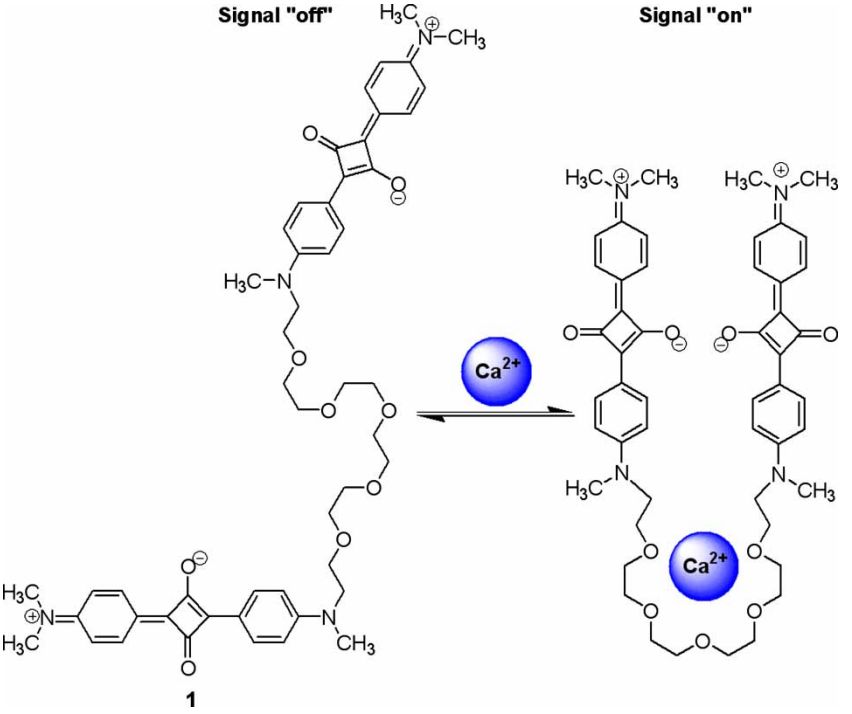

Scheme 2. The colorimetric change is observed upon binding of Ca^{2+} due to the formation of 'H aggregation'.

change brings the two squaraine molecules into close proximity, the 'free' podand has a light-blue colour, which, upon the binding of Ca^{2+}, changes to an intense purple. Cation-driven folding of **1** forms a complex akin to the 'H-aggregation' that is typically observed for squaraine dyes, as the two chromophores are face-to-face stacked (*57*, *58*). Interestingly, this colour change was not seen with the addition of other cations such as Na^{+}, K^{+}, Mg^{2+}, Ba^{2+} or Sr^{2+}, making this receptor selective for Ca^{2+}. Even though this particular example is not targeted towards heavy metals, it is an elegant example of the use of squaraine dyes that have recently appeared in the literature (*59–63*).

Martínez-Máñez and Rurack (*64*) have recently published a paper on the chromogenic signalling of Hg^{2+} in aqueous media, using a squaraine dye containing a dithia–dioxa crown (compound **2a**). The combination of sulphur, oxygen and nitrogen atoms incorporated into the crown backbone has proven to be a highly effective motif in forming Hg^{2+} complexes, and has been incorporated into other colorimetric systems that show efficient signal transduction in optical chemosensing ensembles (*65*). The signalling response is switched 'off' upon the binding of Hg^{2+} within the heterocrown in MeOH–H_2O. Their studies have shown that Hg^{2+} can be detected in concentrations as low as 1×10^{-8} M, depending on the solvent ratio. Other thiophilic cations such as Ag^{+} and Pb^{2+} showed negligible response. The model compound **2b** was also synthesised and showed little response to any of the metals tested under similar experimental conditions.

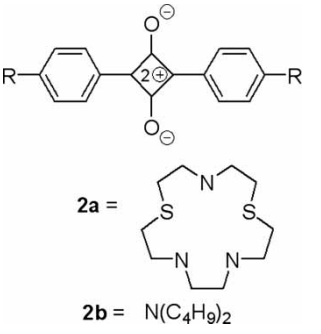

Anslyn and Wallace (*66*) recently published the synthesis of compound **3**, a bidentate ligand that chelates to Fe^{3+} between the deprotonated hydroxyl group on the ortho position of the ring and the carbonyl group of the cyclobutadiene ring. This produces a subtle geometry change as the two negative charges repel one another, thereby producing a colour change and a signal response.

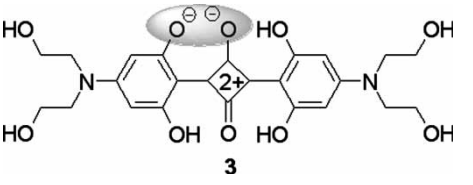

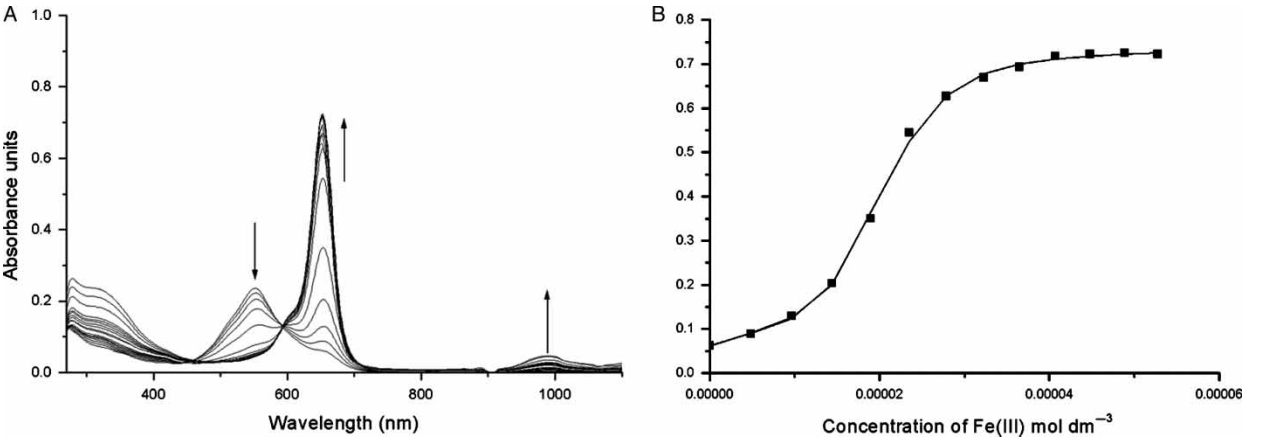

Figure 1. The UV–vis titration spectra (A) and the binding isotherm (B).

It has been shown that the synthesis of an artificial siderophore in the form of a squaraine dye (**3**) is relatively straightforward. The squaraine dye molecule can act as a metal chelator, and is selective for Fe^{3+} at low concentrations (2.3×10^{-5} mol dm^{-3}). The bidentate ligand chelates to Fe^{3+} between the deprotonated hydroxyl group on the ortho position of the ring adjacent to the carbonyl group of the cyclobutadiene ring. This artificial siderophore forms a 2:1 (**3**:metal) complex ($K_a = 10^7\,M^{-1}$) indicative of the sigmoidal isotherm obtained (Figure 1(b)). There is clear evidence in the UV–vis–NIR spectrum that the metal is coordinating to the squaraine ligand from the appearance of the absorption band at 651 nm (Figure 1(a)). One interesting spectroscopic feature that appears in the UV–vis–NIR spectrum for all of the metal titrations is the appearance of another band around 970 nm. This is an unusual band and is clearly a prominent feature in the spectrum. These absorption features are found to be metal–ligand charge transfer (MLCT) or metal–metal charge transfer (MMCT) phenomena. The appearance of this absorption band in the NIR region is good evidence that the squaraine **3** is chelating to the metal ions, and that the MLCT phenomenon is responsible for the hyperchromic shift observed. It has been suggested that the spectroscopic signature for different metal species as each host:metal complex will have a different MMCT band and this is currently being investigated in the Wallace group.

Another interesting metal chelator is compound **6**, developed by Das and colleagues (*67*) who have shown that **6** can act as a metal sensor in an analogous way to the Anslyn and Wallace approach described above. They prepared a novel unsymmetrical cationic squaraine dye (**6**), which has a sharp absorption peak at 782 nm in CH_2Cl_2. The synthesis of unsymmetrical squaraine dyes is an area of interest because of the many potential applications of these

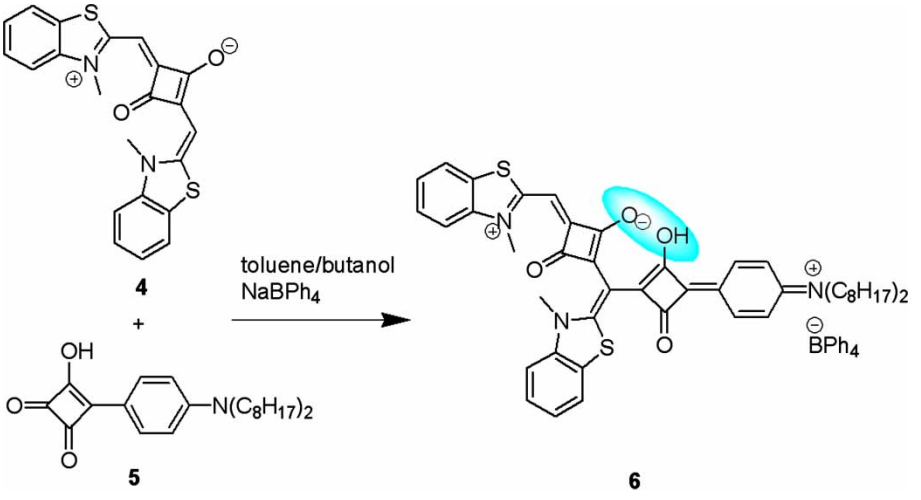

Scheme 3. Synthesis of unsymmetrical squaraine dye **6**.

molecules (*68*). However, a disadvantage of unsymmetrical dyes is the synthetic challenge, as the synthesis is more complicated than the preparation of symmetrical dyes. Dye **6** was synthesised by reacting a semi-squaric acid derivative 3-[4-(*N*,*N*-dioctylamino)phenyl]-4-hydroxycyclobutene-1,2-dione (**5**) with the squarylium dye bis(3-methylbenzothiazol-2-ylidene)squaraine (**4**). Complexation of metal ions such as Hg^{2+} and Pb^{2+} occurs through the oxygen atoms of the central cyclobutane ring (Scheme 3). The binding affinity of **6** with various metal cations (Li^+, Na^+, Mg^{2+}, Ca^{2+}, Ba^{2+}, Zn^{2+}, Cu^{2+} and Pb^{2+}) in CH_2Cl_2 brings about significant changes in its absorption spectrum, resulting in a change in the colour of the solution from green to pink. Mercury(II) showed significant colour changes at concentration levels as low as 49 μM. Molecular modelling calculations suggest that the two oxygen atoms lie in the same plane, because of the strong intramolecular hydrogen bonding interactions. Upon deprotonation, the two negative charges adjacent to one another are twisted out of plane by 63° by electrostatic repulsion.

Ramaiah and colleagues (*69*) utilised the Lewis basic nature of the oxygen atoms on the cyclobutane ring of a squaraine dye **7** (see insert Figure 2) as a binding site to coordinate to metal centres. The ability of compound **7** to act as a bidentate ligand and its potential use as a probe were studied with different metals. The addition of Hg^{2+} resulted in the complete disappearance of the absorbance at 472 nm, leading to a visual colour change from a deep yellow to a colourless solution. Similarly, the addition of 19.8 μM Hg^{2+} to compound **7** gave an eightfold enhancement in fluorescence intensity. This significant turn 'on' intensity led to the visual observation of the change in fluorescence (Figure 2). Job plot and Benesi–Hildebrand analysis have shown 1:1 stoichiometry for the complex with a calculated association constant (K_{ass}) of $4.0 \times 10^4\,M^{-1}$.

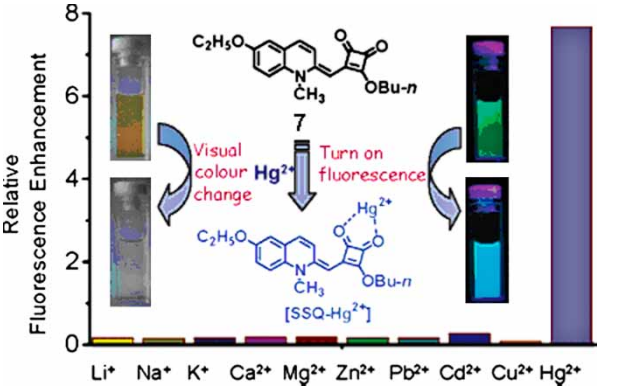

Figure 2. Fluorescence response of **7** towards various metal ions in a mixture (9:1) of water and acetone containing **7** (12 mM). Inset shows visual changes in absorption and fluorescence of **7** with the addition of various metal ions. From left to right: compound **7** alone, metal ions Hg^{2+}, Na^+, Mg^{2+}, Pb^{2+} and Cd^{2+}. Reprinted with permission from Ref. (*69*). Copyright 2008 American Chemical Society.

The electron deficient four-membered cyclobutane ring of the squaraine dye has been utilised by Martínez-Máñez in the development of chromogenic probes for the detection of anions, such as CN^-, and biorelevant thiol-containing species (Scheme 4) (*70*, *71*). They further developed their system to take advantage of the reversible covalent bond to prepare an 'off–on' response, an approach extensively used by Mohr (*72*). Nucleophilic attack of the anion towards **8a** and **8b** turns off the colour, which is regenerated upon the addition of Hg^{2+} (Scheme 4). Interestingly, this dosimeter is shown to be selective towards Hg^{2+} in aqueous systems (Figure 3) (*73*).

While Martínez-Máñez has demonstrated that thiol–squaraine systems work well to detect mercury selectively in aqueous media, the extension of this methodology into

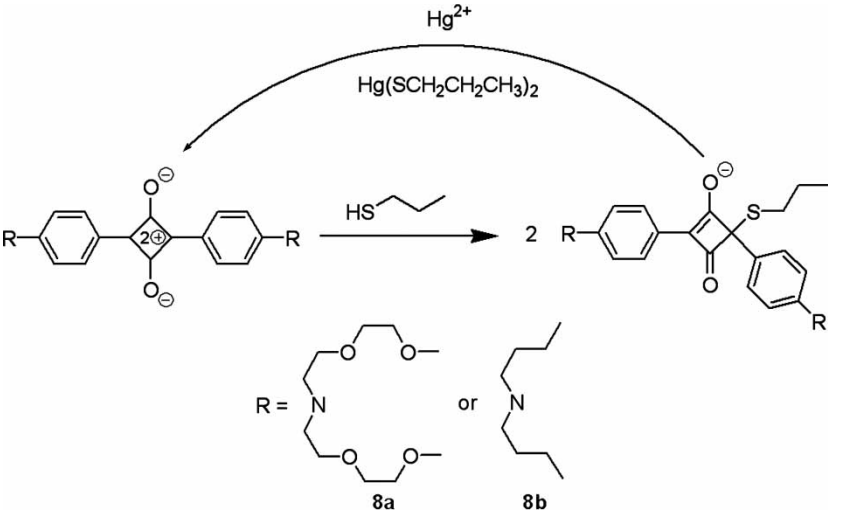

Scheme 4. Squaraine dosimeter **8a** and **8b** can detect Hg^{2+} selectively in aqueous solution.

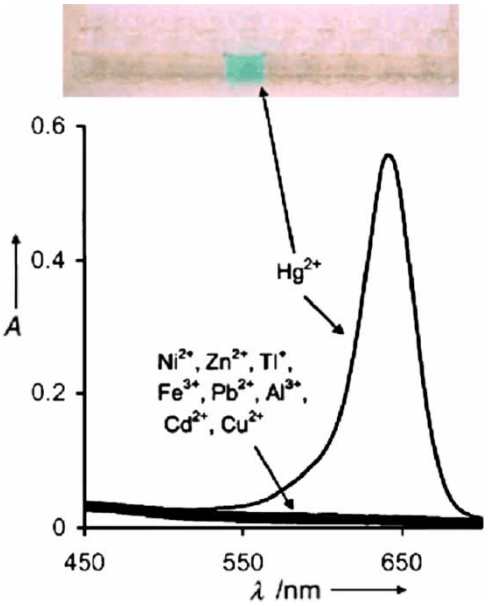

Figure 3. Absorption spectra of **8a** in H_2O-CH_3CN (6×10^{-6} M) at pH 9.6 in CHES buffer, upon the addition of different metal salts (Ros-Lis, J.V.; Marcos, M.D.; Martínez-Máñez, R.; Rurack, K.; Soto, J. *Angew. Chem. Int. Ed. Engl.* **2005**, *44*, 4405–4407. Copyright Wiley-VCH Verlag GmbH & Co KGaA).

organic media has allowed for response to other thiophilic metals. Anslyn and Wallace (*40*) have shown that the squaraine–thiol complex is reversible and have used it to 'scavenge' other thiophilic metals such as palladium in organic media (Scheme 5). Thiol addition had a calculated equilibrium constant (K_{eq}) of $2.9 \times 10^6\,M^{-1}$, with a large entropic and modest enthalpic driving force. This unusual result is attributed to solvent effects arising from a strong coordinative interaction between DMSO and the parent squaraine. It was shown that palladium detection is achieved through thiol scavenging from the **9**–ethanethiol complex leading to a colour 'turn on' of the parent squaraine, analogous to the Martínez-Máñez system. It was found that untreated samples obtained directly from Suzuki couplings showed no response to the assay. One of the disadvantages of palladium detection in Suzuki reactions is that the palladium-catalysed reaction is the large portion of Pd^{2+} converted to its reduced Pd^0 state. This renders the palladium undetectable using this sensor system, due to the formation of palladium black, or coordinated to sterically hindered ligands during the course of the reaction. However, by oxidation or ligand exchange with nitric acid, the soluble nitrate salt $Pd(NO_3)_2$ was formed and could be used to monitor low levels of Pd^{2+} in solution (Figure 4). Treatment of the samples with aqueous nitric acid generates a uniform $Pd(NO_3)_2$ species, which gives an appropriate response. 'Naked-eye' detection of $Pd(NO_3)_2$ was estimated to be as low as 0.5 ppm in solution.

Fluorescein sensors

There are a wide variety of fluorophores that are used as sensors in food safety, environmental quality control and clinical diagnosis (*74*). Xanthene dyes commonly known as fluorescein derivatives or Alexa dyes have become a popular platform for the use as molecular probes. Fluorescein has been used as a fluorescence tag in many biological scenarios due to its excellent water solubility and, depending on the pH, the ability to rise to various fluorescence quantum yields (Scheme 6).

Most of the probes that have incorporated fluorescein are nearly always nonfluorescent before the addition of an analyte, but highly fluorescent upon binding or changes in pH. The mechanism that underlies the fluorescence of fluorescein has been the subject of investigation. It was believed that the carboxylic group of 'traditional'

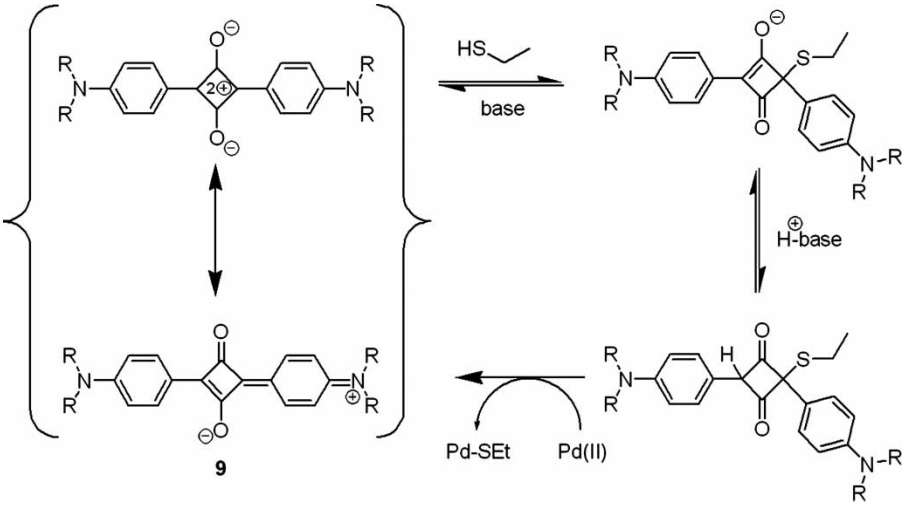

Scheme 5. The decolourisation of **9** with ethanethiol followed by Pd^{2+} scavenging.

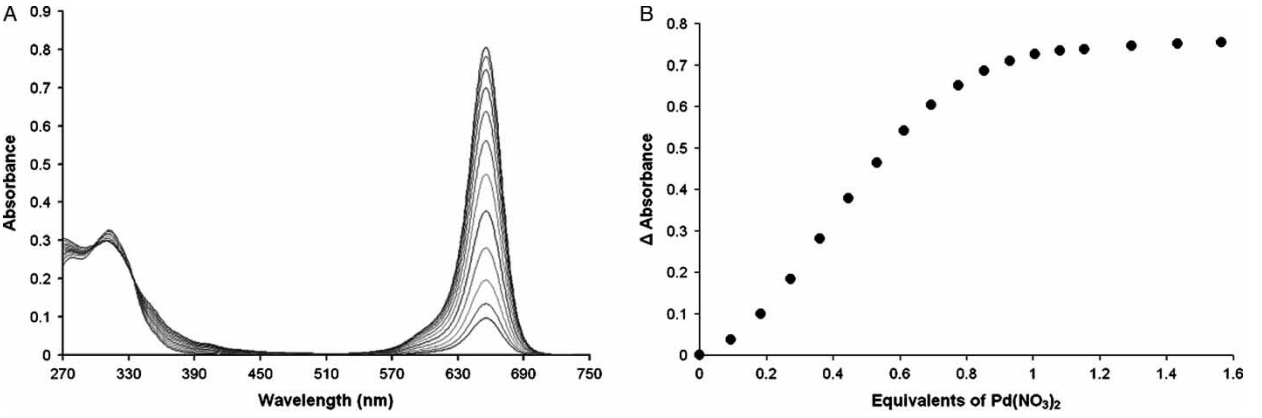

Figure 4. Titration of $Pd(NO_3)_2$ into 8.8×10^{-6} M **9**:SEt in DMSO formulated with ethanethiol and Verkade base. Titration was conducted after 4 h reaction time between squaraine **9** and ethanethiol.

fluorescein dyes was the cause of the fluorescence signal. However, Urano and Nagano (*75*) have recently demonstrated that the absence of the carboxylic group plays no role in fluorescence signal in fluorescein derivatives, despite a report by Lindqvist and Lunden (*76*) who report that the acid group is necessary for strong fluorescence. These findings have led to the development of a plethora of new fluorophores for Zn^{2+} detection.

Lippard et al. (*77–83*) have extensively studied the use of fluorescein derivatives for the imaging of neuronal cell zinc uptake. They have prepared a number of symmetrical fluorescent tertiary amine-based sensors known as the Zinspy family (compounds **10a–10f**).

These compounds exhibit a number of advantages in comparison with previously reported Zn^{2+}-based sensors. These sensors have been found to detect low micromolar levels of Zn^{2+}, they have improved selectivity for Zn^{2+}, they exhibit reversible and rapid Zn^{2+} dissociation, all of the traits desired for the synthesis of good probes. These sensors have elegantly demonstrated the detection and uptake of Zn^{2+} in the living cell, upon some chemical modification by utilising the Lewis acid–base ('soft–soft' interaction) nature of sulphur and mercury atoms, the fluorescein backbone has been designed to detect Hg^{2+} in aqueous solution, for example compound **11**. Each of these molecules contains a single sulphur-binding functional

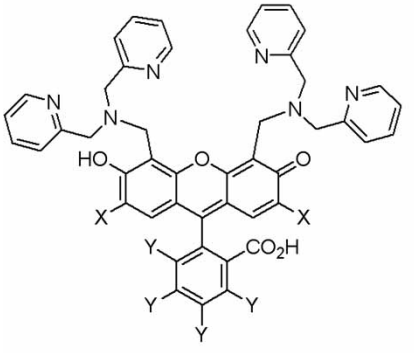

10

10a X = Cl, Y = H
10b X = H, Y = H
10c X = F, Y = H
10d X= Cl, Y = Cl
10e X = Cl, Y = F
10f X = F, Y = F

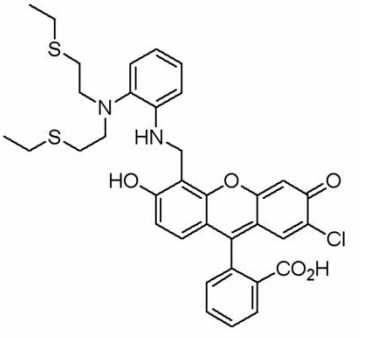

11

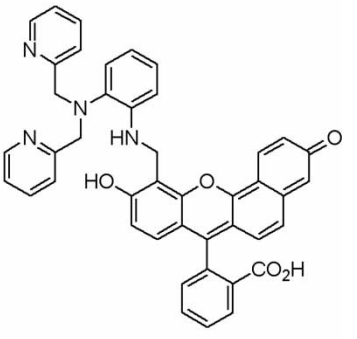

12

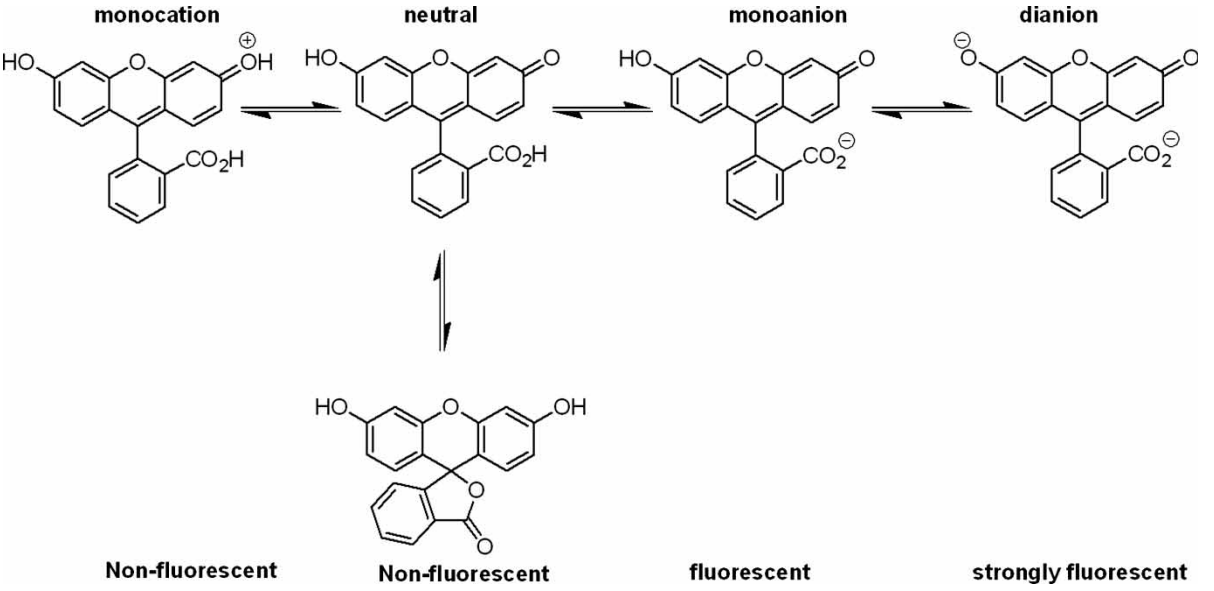

Scheme 6. The different tautomers of fluorescein under different pH conditions. This gives rise to different fluorescein quantum yields.

group that forms 1:1 complexes with Hg^{2+}. The sensitivity was calculated to be in the nanomolar range over other metals (Zn^{2+}, Cd^{2+} Mn^{2+}, Fe^{2+}, Co^{2+} and Cr^{3+}). Compound **11** showed a significant FE in comparison with other metals in aqueous solution. It was previously mentioned that the fluorescence quantum yield is dependent on pH. This is demonstrated in many of Lippard's systems, where, at neutral pH, the florescence emission is quenched by PET due to the lone pair of the aniline moiety (the nitrogen atom has a pK_a of 7.1). Upon the coordination of Hg^{2+}, the fluorescence signal of compound **11** is turned 'on'. As a consequence, Lippard has shown that Hg^{2+} can be detected at concentrations as low as ppb levels in aqueous solution, demonstrating its ability to identify environmentally relevant concentrations of Hg^{2+} (*80*, *84*).

One of the problems of fluorescent probes that are used for *in vivo* detection is the quantitative analysis of trace elements, despite the fact that there are a number of fluorogenic probes that are used as sensors in biological systems (*74*). This is due to variations in excitation intensity, emission collection efficiency, sample thickness and artefacts associated with probe concentration and environment. To overcome this problem, chemosensors

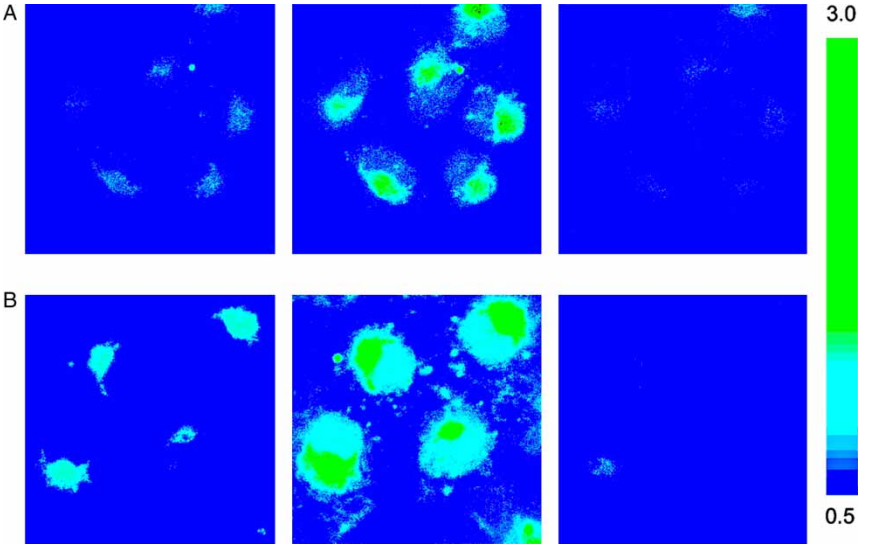

Figure 5. (a) Ratio confocal fluorescence images of live COS-7 cells labelled with **12**, (left), compound **12**-stained cells loaded with 50 μM Zn(pyrithione)2 (centre) and reversal of the cytosolic ratio enhancements with 100 μM TPEN (right). (b) Confocal fluorescence images of NO-triggered release of endogenous Zn^{2+} in live COS-7 cells (left), **12**-stained cells treated with 10 mM SNOC (centre) and reversal of the observed ratio increases with 2 mM TPEN (right). Chang et al. (*77*). 'Copyright 2008 National Academy of Sciences, USA'.

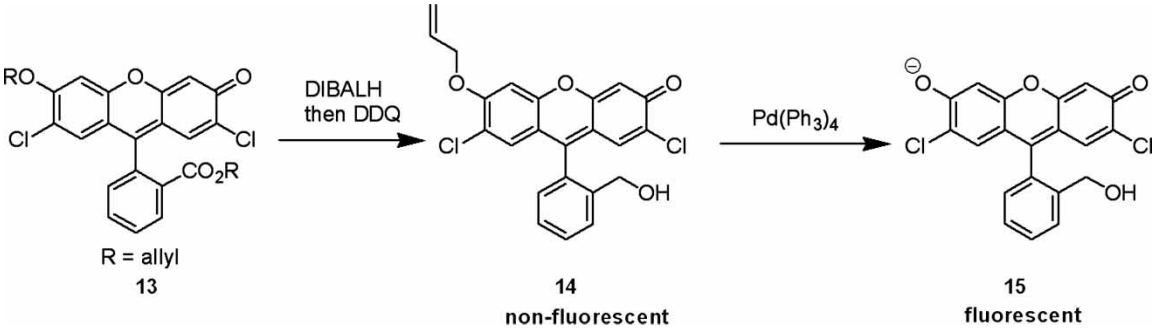

Scheme 7. The Pd-catalyzed transformation of **13** to **14**.

that show a shift in excitation or emission profiles upon complexation can provide accurate and quantitative determinations using ratiometric fluorescence imaging. Lippard and colleagues (*77*) have shown that compound **12** (as the diacetate salt) can permeate the cell and be transformed to fluorescent **12** by the action of intracellular esterases. Ratiometric fluorescence imaging of **12**-stained cells showed that the ratio of fluorescence intensities at 612 and 526 nm for loaded **12**-COS-7 cells (monkey liver cells) reveals that these mammalian cells contain low levels of available ionic Zn^{2+}. Upon the addition of exogenous Zn^{2+} (50 μM), carried into the cell by the ionophore, pyrithione (2-mercaptopyridine *N*-oxide), there was further fluorescence intensity increase. An intriguing aspect of this process is that upon treatment of the cells with the membrane permeable metal ion chelator N,N,N′,N′-tetrakis(2-pyridylmethyl)ethylenediamine (TPEN) (100 μM), there is a reversal of the fluorescent ratio enhancements to baseline levels, suggesting that this probe is reversible (Figure 5(a)).

It is well known that NO plays key roles in intracellular activity, for example, in Zn^{2+} homeostasis, and is an important and versatile signalling molecule (*85*, *86*). To test whether or not compound **12** can detect the release of intracellular Zn^{2+} by NO, Lippard's team treated **12** with the endogenous NO donor *S*-nitrosocysteine (SNOC) and again a FE was observed and was shown to be reversible upon the edition of TPEN (Figure 5(b)).

Fluorescein derivatives are known to be nonfluorescent when the hydroxyl group is alkylated, but they are highly fluorescent when the hydroxyl group is deprotonated. Koide et al. recently published a paper that takes advantage of this fluorescence 'off–on' switch mechanism for the detection of Pd^0 and Pd^{2+}, utilising the Tsuji–Trost reaction in which Pd^0 catalyses the allylic oxidation insertion to cleave the allylic C–O bond of allylic ethers. Koide showed that by attaching an allyl functional group to a fluorescein derivative (compound **13**; Scheme 7), upon reduction of the acid group to the alcohol to form compound **14**, the addition of Pd^0 salts cleaved the allyl functionality to form a highly fluorescent compound **15**. This approach was used for the detection of palladium in pharmaceutical industry samples. Interestingly, other π-philic metals (Ag^+, Ni^{2+}, Au^{3+}, Rh^+, Co^{2+}, Hg^{2+} and Ru^{3+}) did not catalyze the deallylation reaction, Figure 6 (*41*).

Tong et al. synthesised a salicylaldehyde fluorescein hydrazone (compound **16**) that acts as a colorimetric logic chemosensor for pH and Cu^{2+} (*87*); even though this system was not specifically designed to detect metal ions for biological or environmental purposes, it is an example of the use of a fluorescein-derived chemical binary system (*88*). Compound **16** is colourless and exhibits no absorption band above 350 nm regardless of pH. Upon the addition of Cu^{2+}, the lactam moiety of **16** is opened by the formation of a **16**–Cu^{2+} adduct, two absorption peaks appear at around 420 and 502 nm, depending on the pH. If the pH is between 2.5 and 5.0, the absorption band appears at 420 nm for the **16**–Cu^{2+} complex, and increases as the pH increases. If the pH is in the range of 5.0–8.0, a band at 502 nm appears for the same complex, which also increases with increasing pH value. It was demonstrated that all the above absorption spectra responses were reversible (Scheme 8), which was confirmed by the addition of a metal scavenger such as EDTA. The absorption at 502 nm assigned for the **16**–Cu^{2+} complex (pH $>$ 5.0) has a stronger (more intense) signal than the band observed at 420 nm (pH $<$ 5.0). The absorbance at 502 nm at pH 8.0 was nearly six times larger than that at 420 nm (pH $<$ 5.0). Based on this observation,

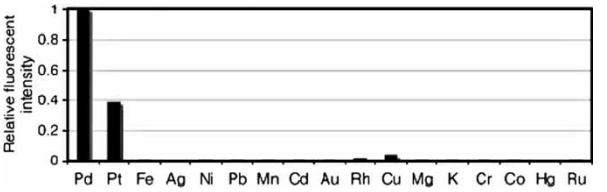

Figure 6. Metal specificity: Pd^{2+}, Pt^{2+}, Fe^{3+}, Ag^+, Ni^{2+}, Pb^{2+}, Mn^{2+}, Cd^{2+}, Au^{3+}, Rh^+, Cu^{2+}, Mg^{2+}, K^+, Cr^{3+}, Co^{2+}, Hg^{2+} and Ru^{3+}. Reprinted with permission from Ref. (*41*). Copyright 2008 American Chemical Society.

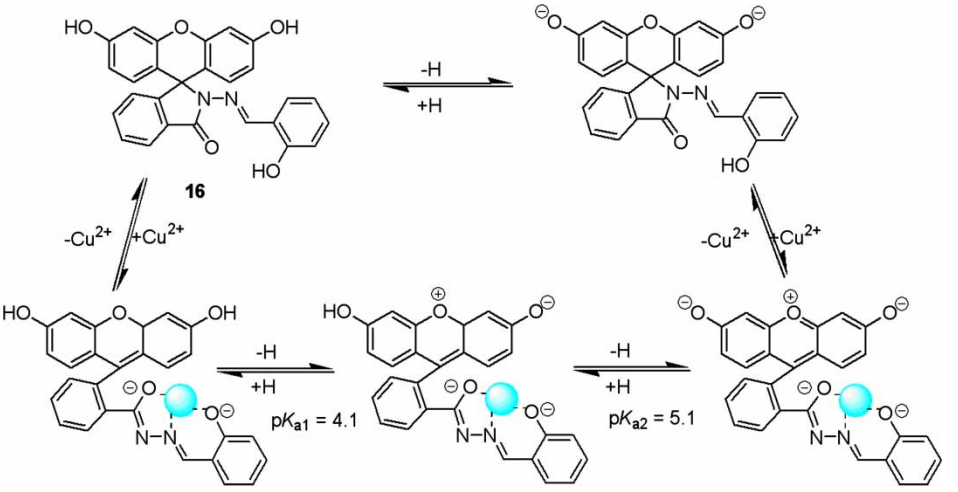

Scheme 8. Proton dissociation of **Cu^{2+}–16**, Cu^{2+} is represented by the blue sphere.

compound **16** was capable of acting as a colorimetric logic gate (Table 1). $Input_1$ and $Input_2$ represent the presence of Cu^{2+} and H^+, respectively. The lack of Cu^{2+} gives an $input_1$ state of '0', i.e., the solution was colourless and there was no absorption at the wavelength range of 350–600 nm. When the concentration of Cu^{2+} was high enough ($\geq 1\ \mu M$) an $input_1$ state of '1' is achieved, and the system responded to the environmental pH change with a colour change. In the presence of Cu^{2+} and a pH $\leq$ 5.0 ($input_2$ state '1'), the system generated a Cu^{2+}-driven YES logic gate giving the output signal ($Output_{410\,nm}$) with the 'on' state whereby the absorbance is >0.05 absorbance units; when pH was increased further to pH > 5.0 ($input_2$ state '0'), the system turned to an INHIBIT logic gate (essentially the integration of an AND and NOT logic gates, where the NOT is applied to only one of the inputs), giving the output signal ($Output_{502\,nm}$) with the 'on' state greater than 0.1 absorbance units (Figure 7). Orange is seen more easily by individuals and therefore an orange colour is seen when outputs at 410 and 502 are in the 'on' or '1' state simultaneously.

Table 1. Truth table for **16**–Cu^{2+} INHIBIT logic system.

$Input_1$ Cu^{2+}	$Input_2$ H	$Output_{410\,nm}$	$Output_{502\,nm}$
0	0	0	0
0	1	0	0
1	0	1	1
1	1	1	0

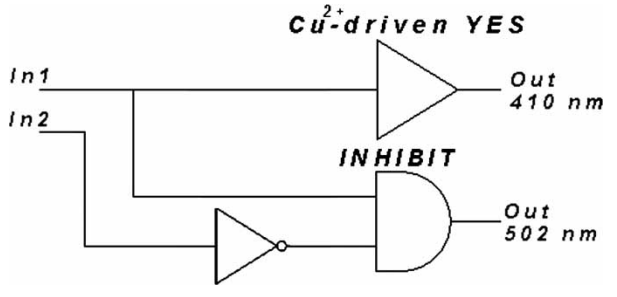

Figure 7. The operation of a Cu^{2+}-driven YES ($Output_{410\,nm}$) and-INHIBT ($Output_{502\,nm}$) integrated logic gate. The input elements for the addition of Cu^{2+} and pH are represented as In_1 and In_2, respectively.

Other dyes

Canary et al. synthesised a tripodal N4 ligand that contains 8-hydroxyquinoline, a well-known chromophore that has been used extensively as an analytical tool for sensing Zn^{2+} (compound **17**) (*82*). Compound **17** showed excellent 1:1 binding stoichiometry and strong sensitivity to Zn^{2+}. The 1:1 binding motif was also confirmed by single crystal X-ray crystallography (Scheme 9). Again, the signal motif is observed by the strong FE upon the addition of Zn^{2+}, like some of the previous sensors highlighted in this review; the nitrogen atoms lone pair PET quenches the fluorescence signal. Upon the addition of the zinc salt, the Lewis acid–base adduct enhanced the fluorescence. A series of metal solutions showed subpicomolar sensitivity, with a detection limit of compound **17** reported to be in the range of 10 fM to 1 pM ($\log K_1 = 13.29$) in HEPES-buffer solution. What is noteworthy about this study is the use of time-resolved fluorescence spectroscopy (TRF), a technique that is emerging as a valuable tool for cell imaging. TRF can be used to measure different fluorescence signals of fluorophores with different lifetimes. Canary's study showed that TRF cannot only provide accurate

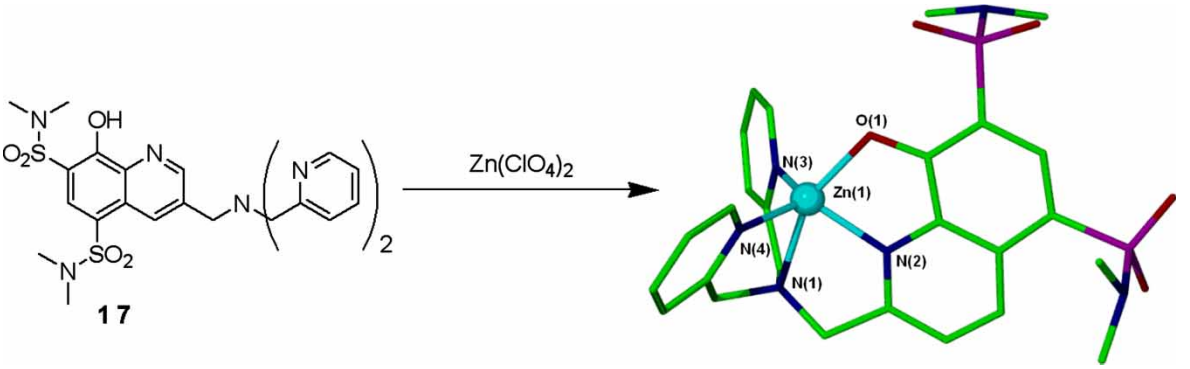

Scheme 9. The synthesis of **17** and the X-ray crystal structure, highlighting a 1:1 host–guest binding.

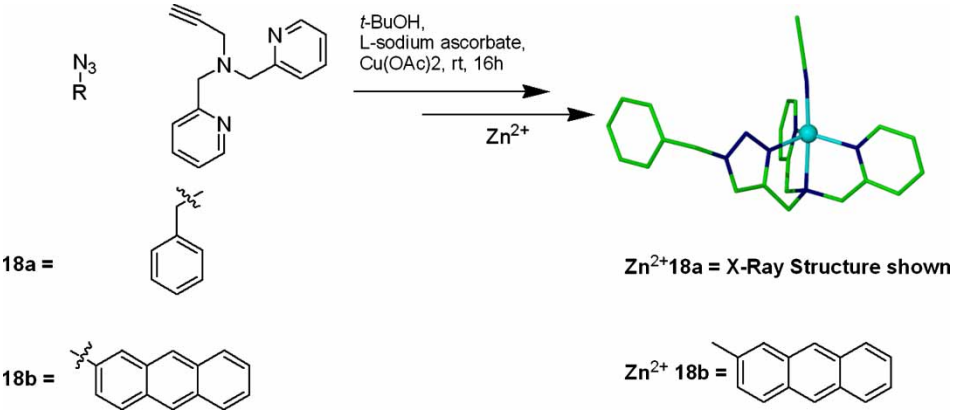

Scheme 10. Synthesis of compound **18b** and X-ray crystal structure showing the N3-anchored five-membered coordination rings.

detection of Zn^{2+}, but can also discriminate between other fluorescent forms of compound **17** and its metal complex. Therefore, in biological systems, TRF can be used to monitor Zn^{2+} under different environmental conditions.

One disadvantage of many of the reported receptors is the multistep synthetic procedures required to produce them. However, the application of the Cu^{+}-catalyzed Huisgen cycloaddition reaction, commonly referred to as the 'click' reaction, is appearing more often in the design and synthesis of molecular receptors. Recently, Zhu and colleagues (*88*) has taken advantage of the ease of the 'click' approach to synthesise a number of 1,2,3-triazolyl compounds (imidazolyl mimics), for example, compound **18a** and compound **18b,** the later contains an anthracene moiety as the singling motif (Scheme 10). Compound **18b** was shown to detect nanomolar levels of Zn^{2+} under physiological conditions K_d/nM = 12 by monitoring the increase of the fluorescence quantum yield that increased approximately eight times and modelling the host–guest interaction on a 1:1 model (Figure 8).

Another interesting chemosensor developed by Qian and colleagues (*90*) is based on a 4-aminonaphthalinide group that has been used as a fluoroionophore, compound **19**. Receptor **19** was synthesised from the reaction of 2,6-bis-(chloromethyl)pyridine and *N*-[2-(2-hydroxethoxy)-ethyl]4-piperazino-1,8-naphthalimide. This water-soluble dye showed a remarkable fluorescence 'turn on' when coordinated to Hg^{2+}. Receptor **19** adopts a molecular cleft motif, whereby the nitrogen atoms act as the binding sites for the metal cations. Qian showed that the nitrogen atoms in compound **19** can PET quench the fluorescence signal ($\Phi = 0.007$, $\lambda_{em} = 548$ nm); upon the addition of a target species, a FE is seen, for example $\Phi/\Phi_0 = 17.4$ upon the addition of Hg^{2+}, in comparison with all of other metals studied (Figure 9). The selectivity of Hg^{2+} over a number of other metals still holds true, as competitive experiments had little or no effect on the FE. This was demonstrated by mixing a number of metal salts together, where no signal amplification was seen until the addition of Hg^{2+}, concluding that compound **19** showed remarkable selectivity towards Hg^{2+} in complex mixtures.

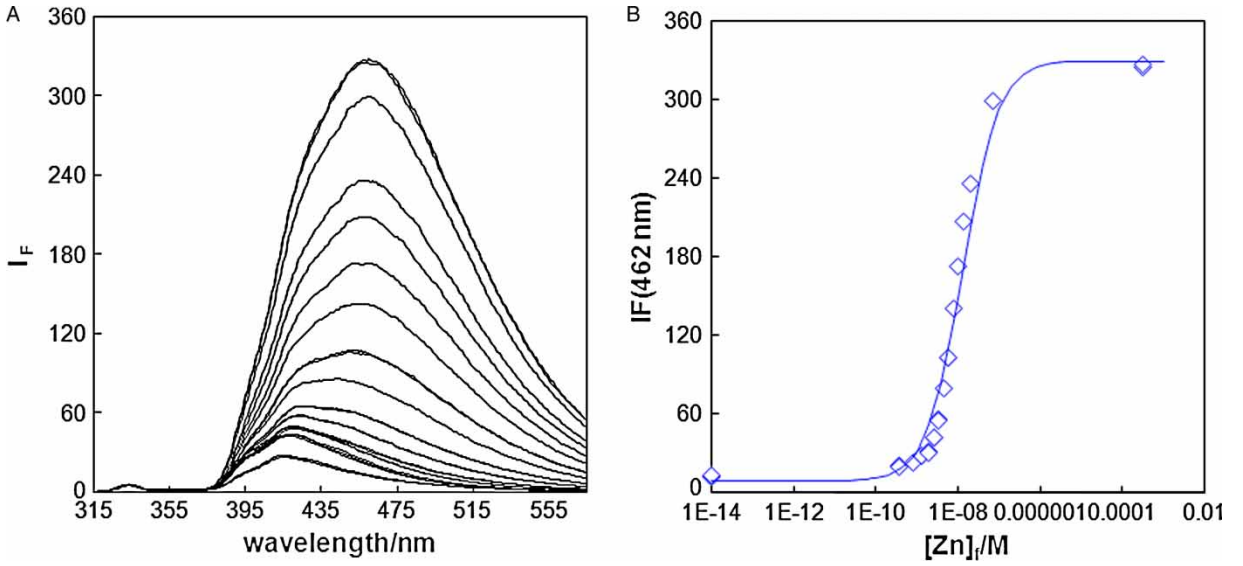

Figure 8. (a) Fluorescence spectra (λ_{ex} = 330 nm) of **18b** (4.9 μM) in H_2O (HEPES: 50 mM, pH 7.2; KNO_3: 100 mM; ethylene glycol tetraacetic acid (EGTA): 10 mM) upon the addition of zinc triflate at 25°C, (b) fluorescence binding isotherm (modelled on a 1:1 curve fitting equation).

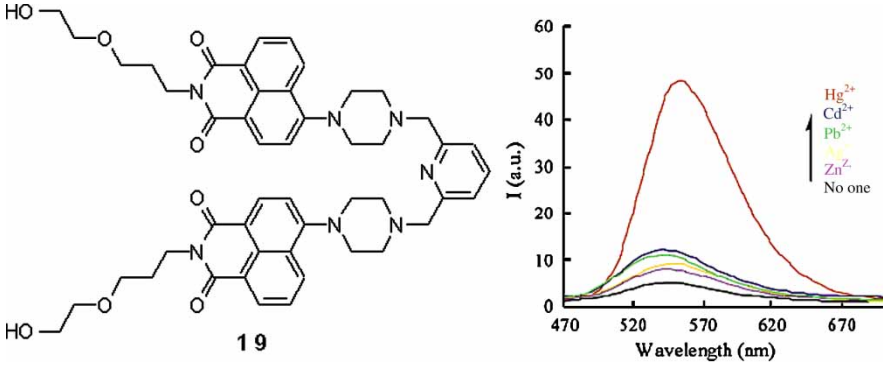

Figure 9. Fluorescence spectra of compound **19** (1.0×10^{-5} M) in Tris–HCl buffer (0.01 M solution (EtOH:H_2O = 1:9 v/v, pH 6.98) in the presence of different metal ions (5.0×10^{-5} M), and nearly no response to some other metal ions (Mg^{2+}, Ca^{2+}, K^+, Fe^{3+}, CO^{2+}, Cu^{2+} and Ni^{2+}). Reprinted with permission from Ref. (*90*). Copyright 2008 American Chemical Society.

Conclusions

The topic of heavy metal detection is a vast subject area and a research thrust that seems to be a continuing endeavour for many scientists worldwide. This mini-review has covered some of the most recent developments in sensor design in terms of the host–guest recognition process reported between 2004 and 2008, in particular, the squaraine and fluorescein derivatives. The author sincerely apologises to all of those whose work could not be included in this mini-review because of space constraints, for example, Chang and colleagues (*91–93*) who have developed a number of small molecule sensor motifs, one elegant example is the incorporation of a BODIPY motif, for the detection of Pb^{2+}, Hg^{2+} and Cu^{2+}. Since this article has been in press Lippard has just published an elegant review on the detection of mercuric ion, using various different molecular dyes *(94)*.

Acknowledgements

The author would like to thank the organisers (Profs Eric V. Anslyn and Jonathan Sessler) of the 2008 IMSIC held in Las Vegas for the invitation to write a mini-review for the special edition of *Supramolecular Chemistry* in honour of this event. The author would also like to thank the University of Southern Mississippi and the Southeastern Regional Research Initiative (Grant Number 4000055830) for funding the ongoing research in the Wallace Laboratory.

References

(1) Tautkus, S.; Steponeniene, L.; Kazlauskas, R. *J. Serb. Chem. Soc.* **2004**, *69*, 393–402.
(2) Gondal, M.A.; Hussain, T.; Yamani, Z.H.; Baig, M.A. *Talanta* **2006**, *69*, 1072–1078.
(3) Zejli, H.; Hidalgo-Hidalgo de Cisneros, J.L.; Naranjo-Rodriguez, I.; Elbouhouti, H.; Choukairi, M.; Bouchta, D.; Temsamani, K.R. *Anal. Lett.* **2007**, *40*, 2788–2798.
(4) Yang, L.; McRae, R.; Henary, M.M.; Patel, R.; Lai, B.; Vogt, S.; Fahrni, C.J. *Proc. Natl Acad. Sci. USA* **2005**, *102*, 11179–11184.
(5) Gila, L.; Barat, J.M.; Garcia-Breijo, E.; Ibañez, J.; Martínez-Máñez, R.; Soto, J.; Llobet, E.; Brezmes, J.; Aristoy, M.-C.; Toldrá, F. *Sens. Actuat. B* **2008**, *131*, 362–370.
(6) de Silva, A.P.; Gunaratne, H.Q.N.; Gunnlaugsson, T.; Huxley, A.J.M.; McCoy, C.P.; Rademacher, J.T.; Rice, T.E. *Chem. Rev.* **1997**, *97*, 1515–1566.
(7) Leonard, J.P.; Nolan, C.B.; Stomeo, F.; Gunnlaugsson, T. *Top. Curr. Chem.* **2007**, *281*, 1–43.
(8) Shortreed, M.; Kopelman, R.; Kuhn, M.; Hoyland, B. *Anal. Chem.* **1996**, *68*, 1414–1418.
(9) Basabe-Desmonts, L.; Reinhoudt, D.N.; Crego-Calama, M. *Chem. Soc. Rev.* **2007**, *36*, 993–1017.
(10) Crichton, R.R. *Inorganic Biochemistry of Iron Metabolism: From Molecular Mechanisms to Clinical Consequences*; John Wiley & Sons: New York, 2001.
(11) Raymond, K.; Carran, C.J. *Acc. Chem. Res.* **1979**, *12*, 183–190.
(12) Hider, R.C.; Liu, Z.D. *Siderophores*; Dekker: New York, 2004.
(13) Frederickson, C.J.; Giblin, L.J.; Krezel, A.; McAdoo, D.J.; Muelle, R.N.; Zeng, Y.; Balaji, R.V.; Masalha, R.; Thompson, R.B.; Fierke, C.A.; et al. *Exp. Neurol.* **2006**, *198*, 285–293.
(14) Frederickson, C.J.; Giblin, L.J.; Rengarajan, B.; Masalha, R.; Frederickson, C.J.; Zeng, Y.P.; Lopez, E.V.; Koh, J.Y.; Chorin, U.; Besser, L.; Hershfinkel, M.; et al. *J. Neurosci. Methods* **2006**, *154*, 19–29.
(15) Frederickson, C.J.; Koh, J.Y.; Bush, A.I. *Nat. Rev. Neurosci.* **2005**, *6*, 449–462.
(16) Berg, J.M.; Shi, Y.G. *Science* **1996**, *271*, 1081–1085.
(17) Vallee, B.L.; Falchuk, K.H. *Physiol. Rev.* **1993**, *73*, 79–118.
(18) Smith, M.A.; Harries, P.L.R.; Sayre, L.M.; Perry, G. *Proc. Natl Acad. Sci. USA* **1997**, *94*, 9866–9868.
(19) Frederickson, C.J. *Int. Rev. Neurobiol.* **1989**, *31*, 145–238.
(20) Zalewski, P.D.; Millard, S.H.; Forbes, I.J.; Kapaniris, O.; Slavotinek, A.; Betts, W.H.; Ward, A.D.; Lincoln, S.F.; Mahadevan, I. *J. Histochem. Cytochem.* **1994**, *42*, 877–884.
(21) Sorenson, M.B.; Stoltenberg, M.; Juhl, S.; Danscher, G.; Ernst, E. *Prostate* **1997**, *31*, 125–130.
(22) Martin, J.H.; Coale, K.H.; Johnson, K.S.; Fitzwater, S.E.; Gordon, R.M.; Tanner, S.J.; Hunter, C.N.; Elrod, V.A.; Nowicki, J.L.; Coley, T.L.; et al. *Nature* **1994**, *371*, 123–129.
(23) Dumford, B.E. In *Proceedings NATO Advanced Study Institute*; Reed, C.A., Ed.; Reidal: Dordrect, 1982; pp. 25–42.
(24) Boyd, P.W.; Law, C.S.; Wong, C.S.; Nojiri, Y.; Tsuda, A.; Levasseur, M.; Takeda, S.; Rivkin, R.; Harrison, P.J.; Strzepek, R.; et al. *Nature* **2004**, *428*, 549–553.
(25) Boyd, P.W.; Watson, A.J.; Law, C.S.; Abraham, E.R.; Trull, T.; Murdoch, R.; Bakker, D.C.; Bowie, A.R.; Buesseler, K.O.; Chang, H.; et al. *Nature* **2000**, *407*, 695–702.
(26) Tsuda, A. *Science* **2003**, *300*, 958–961.
(27) Wells, M.L.; Mayer, L.M.; Guillard, R.R.L. *Mar. Ecol. Prog. Ser.* **1991**, *69*, 93–102.
(28) Wells, M.L.; Mayer, L.M. *Mar. Chem.* **1991**, *32*, 195–210.
(29) Wolfe, M.F.; Schwarzbach, S.; Sulaiman, R.A. *Environ. Toxicol. Chem.* **1998**, 146–160.
(30) Magos, L. *Met. Ions Bio. Syst.* **1997**, *34*, 321–370.
(31) von Burg, R.J. *J. Appl. Toxicol.* **1995**, *15*, 483–494.
(32) Liesen, P.J.; Varma, R.S.; Naicker, K.P. *Tetrahedron Lett.* **1999**, *40*, 2075–2078.
(33) Liu, W.-J.; Xie, Y.-X.; Liang, Y.; Li, J.-H. *Synthesis* **2006**, 860–864.
(34) Baxter, J.M.; Steinhuebel, D.; Palucki, M.; Davis, I.W. *Org. Lett.* **2005**, *7*, 215–218.
(35) Bushwald, S.L.; Mauger, C.; Miganai, G.; Scholz, U. *Adv. Synth. Catal.* **2006**, *61*, 23–39.
(36) Zeni, G.; Larock, R.C. *Chem. Rev.* **2004**, *104*, 2285–2309.
(37) Tietze, L.F.; Ila, H.; Bell, H.P. *Chem. Rev.* **2004**, *104*, 3453–3516.
(38) Nicolaou, K.C.; Bulger, P.G.; Sarlah, D. *Angew. Chem., Int. Ed.* **2005**, *44*, 4490–4527.
(39) Arvela, R.K.; Leadbeater, N.E.; Collins, M.J. *Tetrahedron.* **2005**, *61*, 9349–9355.
(40) Houk, R.J.T.; Wallace, K.J.; Hewage, H.S.; Anslyn, E.V. *Tetrahedron* **2008**, *64*, 8271–8278.
(41) Song, F.; Garner, A.L.; Koide, K. *J. Am. Chem. Soc.* **2007**, *129*, 12354–12355.
(42) Lee, D.Y. K.; Lam, M.H. W.; Wong, W.-Y. *New J. Chem.* **2002**, *26*, 330–335.
(43) Aragoni, M.C.; Arca, M.; Demartin, F.; Devillanova, F.A.; Isaia, F.; Garau, A.; Lippolis, V.; Jalali, F.; Papke, U.; Shamsipur, M.; et al. *Inorg. Chem.* **2002**, *41*, 6623–6632.
(44) Hartley, J.H.; James, T.D.; Ward, C.J. *J. Chem. Soc., Perkin Trans. 1* **2000**, 3155–3185.
(45) Elliott, E.K.; Hu, J.; Gokel, G.W. *Supramol. Chem.* **2007**, *19*, 175–183.
(46) Gokel, G.W.; Carasel, I.A. *Chem. Rev.* **2007**, *36*, 378–389.
(47) Gokel, G.W.; Leevy, W.M.; Weber, M.E. *Chem. Rev.* **2004**, *104*, 2723–2750.
(48) Law, K.-Y. *Chem. Rev.* **1993**, *93*, 449–486.
(49) Sreejith, S.; Carol, P.; Chithra, P.; Ajayaghosh, A. *J. Mater. Chem.* **2008**, *18*, 264–274.
(50) Schmidt, H.A. *Synthesis* **1980**, 961–994.
(51) Anslyn, E.V. *Org. Lett.* **2007**, *9*, 1627–1629.
(52) Ajayaghosh, A. *Chem. Soc. Rev.* **2003**, *32*, 181–191.
(53) Ajayaghosh, A. *Acc. Chem. Res.* **2005**, *38*, 449–459.
(54) Ajayaghosh, A.; Arunkumar, E. *Org. Lett.* **2005**, *7*, 3135–3138.
(55) Arunkumar, E.; Ajayaghosh, A.; Daub, J. *J. Am. Chem. Soc.* **2005**, *127*, 3156.
(56) Pedersen, C.J. *J. Am. Chem. Soc.* **1967**, *89*, 7017–7036.
(57) Chen, H.; Law, K.-Y.; Perlstein, J.; Whitten, D.G. *J. Am. Chem. Soc.* **1995**, *117*, 7257–7258.
(58) Tian, M.; Furuki, M.; Iwasa, I.; Sato, Y.; Pu, L.S.; Tatsuura, S. *J. Phys. Chem. B* **2002**, *106*, 4370–4376.
(59) Gassensmith, J.J.; Arunkumar, E.; Barr, E.; Baumes, J.M.; DiVittorio, K.M.; Johnson, J.R.; Noll, B.C.; Smith, B.D. *J. Am. Chem. Soc.* **2007**, *129*, 15054–15059.
(60) Basheer, M.C.; Santhosh, U.; Alex, S.; Thomas, K.G.; Suresh, C.H.; Das, S. *Tetrahedron* **2007**, *63*, 1617–1623.
(61) Snee, P.T.; Somers, R.C.; Nair, G.; Zimmer, J.P.; Bawendi, M.G.; Nocera, D.G. *J. Am. Chem. Soc.* **2007**, *128*, 13320–13321.

(62) Tatarets, A.L.; Fedyunyayeva, I.A.; Dyubko, T.S.; Povrozin, Y.A.; Doroshenko, A.O.; Terpetschnig, E.A.; Patsenker, L.D. *Anal. Chem. Acta* **2006**, *570*, 214–223.
(63) Sheng-Yao, H.; Chien-Chen, L.; Yi-Hung, L.; Shie-Ming, P.; Sheng-Hsien, C. *Angew. Chem., Int. Ed. Engl.* **2007**, *46*, 2013–2017.
(64) Ros-Lis, J.V.; Martínez-Máñez, R.; Rurack, K.; Sancenon, F.; Soto, J.; Spieles, M. *Inorg. Chem.* **2004**, *43*, 5183–5185.
(65) Jiménez, D.; Martínez-Máñez, R.; Sancenón, F.; Soto, J. *Tetrahedron Lett.* **2004**, 1257–1259.
(66) Wallace, K.J.; Gray, M.; Zhong, Z.; Lynch, V.M.; Anslyn, E.V. *Dalton Trans.* **2005**, 2436–2441.
(67) Basheer, M.C.; Alex, S.; George Thomas, K.G.; Suresh, C.H.; Das, S. *Tetrahedron* **2006**, *62*, 605–610.
(68) Tatarets, A.L.; Fedyunyaeva, I.A.; Terpetschnig, E.; Patsenker, L.D. *Dyes Pigments* **2005**, *64*, 125–134.
(69) Avirah, R.R.; Jyothish, K.; Ramaiah, D. *Org. Lett.* **2007**, *9*, 121–124.
(70) Ros-Lis, J.V.; García, B.; Jiménez, D.; Martínez-Máñez, R.; Sancenón, F.; Soto, J.; Gonzalvo, F.; Valldecabres, M.C. *J. Am. Chem. Soc.* **2004**, *126*, 4064–4065.
(71) Ros-Lis, J.V.; Martínez-Máñez, R.; Soto, J.; Gonzalvo, F. *Chem. Commun.* **2002**, 2248–2249.
(72) Mohr, G.J. *Chem. Eur. J.* **2004**, *10*, 1082–1090.
(73) Ros-Lis, J.V.; Marcos, M.D.; Martínez-Máñez, R.; Rurack, K.; Soto, J. *Angew. Chem., Int. Ed.* **2005**, *44*, 4405–4407.
(74) Panchuk-Voloshina, N.; Haugland, R.P.; Bishop-Stewart, J.; Bhalgat, M.K.; Millard, P.J.; Mao, F.; Leung, W.Y.; Haugland, R.P. *J. Histochem. Cytochem.* **1999**, *47*, 1179–1188.
(75) Urano, Y.; Kamiya, M.; Kanda, K.; Ueno, T.; Hirose, K.; Nagano, T. *J. Am. Chem. Soc.* **2005**, *127*, 4888–4894.
(76) Lindqvist, L.; Lunden, G.W. *J. Phys. Chem.* **1966**, *44*, 1711–1722.
(77) Chang, C.J.; Jaworski, J.; Nolan, E.M.; Sheng, M.; Lippard, S.J. *Proc. Natl Acad. Sci. USA* **2004**, *101*, 1129–1134.
(78) Nolan, E.M.; Jaworski, J.; Racine, M.E.; Sheng, M.; Lippard, S.J. *Inorg. Chem.* **2006**, *45*, 9748–9757.
(79) Nolan, E.M.; Lippard, S.J. *J. Am. Chem. Soc.* **2007**, *129*, 5910–5918.
(80) Nolan, E.M.; Racine, M.E.; Lippard, S.J. *Inorg. Chem.* **2006**, *45*, 2742–2749.
(81) Nolan, E.M.; Ryu, J.W.; Jaworski, J.; Feazell, R.P.; Sheng, M.; Lippard, S.J. *J. Am. Chem. Soc.* **2006**, *128*, 15517–15528.
(82) Royzen, M.; Durandin, A.; Young, Jr., V.G.; Geacintov, N.E.; Canary, J.W. *J. Am. Chem. Soc.* **2006**, *128*, 3854–3855.
(83) Woodroofe, C.C.; Lippard, S.J. *J. Am. Chem. Soc.* **2003**, *125*, 11458–11459.
(84) Nolan, E.M.; Lippard, S.J. *J. Am. Chem. Soc.* **2003**, *125*, 14270–14271.
(85) Kroncke, K.-D.; Kolb-Bachofen, V. *Meth. Enzymol.* **1991**, *301*, 126–145.
(86) Spahl, D.U.; Berendji-Grün, D.; Suschek, C.V.; Kolb-Bachofen, V.; Kröncke, K.-D. *Proc. Natl Acad. Sci. USA* **2003**, *100*, 13952–13957.
(87) Chen, X.; Li, Z.; Xiang, Y.; Tong, A. *Tetrahedron Lett.* **2008**, *49*, 4697–4700.
(88) Atwood, J.L.; Steed, J.W. In *Encyclopedia of Supramolecular Chemistry*; Brown, G.J., de Silva, A.P., Weir, S.M., Eds.; Taylor & Francis: New York, 2004; pp. 893–901.
(89) Huang, S.; Clark, R.J.; Zhu, L. *Org. Lett.* **2007**, *9*, 4999–5002.
(90) Guo, X.; Qian, X.; Jia, L. *J. Am. Chem. Soc.* **2004**, *126*, 2272–2273.
(91) Zeng, L.; Miller, E.W.; Pralle, A.; Isacoff, E.Y.; Chang, C.J. *J. Am. Chem. Soc.* **2006**, *128*, 10–11.
(92) Yoon, S.; Albers, A.E.; Wong, A.P.; Chang, C.J. *J. Am. Chem. Soc.* **2005**, *127*, 16030–16031.
(93) He, Q.; Miller, E.W.; Wong, A.P.; Chang, C.J. *J. Am. Chem. Soc.* **2006**, *128*, 9316–9317.
(94) Nolan, E.M.; Lippard, S.J. *Chem. Rev.* **2008**, *108*, 3443–3480.